Elaboration and Electrical Characterization of Langmuir−Blodgett Films of 4-Mercaptoaniline Functionalized Platinum Nanoparticles

H. Perez,*,† R. M. Lisboa de Sousa,† J-P. Pradeau,† and P-A. Albouy‡

CEA DSM/DRECAM, Service de Chimie Moléculaire, Bât. 125, 91191 Gif s/Yvette, France, and Laboratoire de Physique des Solides (U.M.R. 8502), Bât. 510, Université de Paris-Sud, 91405 Orsay, France

Received September 27, 2000. Revised Manuscript Received December 15, 2000

The elaboration of Langmuir−Blodgett (LB) films of platinum nanoparticles is described. In contrast to most of the previously reported studies that concern metallic particles capped with long alkyl chains, the aggregates involved in this work bear external polar amine functions. The area per particle is consistent with the formation of essentially monoparticle thick Langmuir films at low surface pressures. Pure films of these particles are efficiently transferred horizontally whereas conventional vertical deposition can be used with mixed films containing added fatty acid. The LB films were characterized by IR spectroscopy, AFM, STEM, and X-ray diffraction. The electrical properties of the ultrathin materials based on pure films and mixed films were investigated. The nonmetallic conductivity is characterized by an activation energy of ≈80 meV and lies in the range 10^{-2} to 10^{-3} S·cm^{-1}. The material exhibits good long-term electrical stability. Finally, it is shown that the fatty acid can be washed out from mixed films without dramatic effects on the conductivity of the material.

1. Introduction

Many improvements have been made since the middle of the 1990s in the synthesis of metal or semiconductor nanoparticles. The ability to elaborate in a reproducible manner organically capped colloidal particles with a diameter of a few nanometers and a narrow size distribution allows them to be handled as molecules[1] for building nanostructured materials: for instance, it is possible to obtain stable suspensions so that methods such as self-assembly or Langmuir−Blodgett techniques can be used for the elaboration of thin films.[2−6] Along these lines, we recently described the synthesis of platinum nanoparticles functionalized with 4-mercaptoaniline that are soluble in dimethyl sulfoxide.[7] We report in the present paper on their use for building Langmuir and Langmuir−Blodgett films. The formation of monoparticle thick films is discussed and related to structural features of the bulk material. The electrical properties of these ultrathin materials are investigated.

* To whom correspondence should be addressed.
† CEA DSM/DRECAM.
‡ Université de Paris-Sud.

(1) Brust, M.; Bethell, W. M.; Schiffrin, D. J.; Whyman, R. *J. Chem. Soc. Chem. Commun.* **1994**, 801.
(2) Murray, C. B.; Kagan, C. R.; Bawendi, M. G. *Science* **1995**, *270*, 1335.
(3) Freeman, R. G.; Grabar, K. C.; Allison, K. J.; Bright, R. M.; Davis, J. A.; Guthrie, A. P.; Hommer, M. B.; Jackson, M. A.; Smith, P. C.; Walter, D. G.; Natan, M. J. *Science* **1995**, *267*, 1629.
(4) Heath, J. R.; Knobler, C. M.; Leff, D. V. *J. Phys. Chem. B* **1997**, *101*, 189.
(5) Motte, L.; Pileni, M. P. *J. Phys. Chem. B* **1998**, *102*, 4104.
(6) Dabousi, B. O.; Murray, C. B.; Rubner, M. F.; Bawendi, G. *Chem. Mater.* **1994**, *6*, 216.
(7) Perez, H.; Pradeau, J.−P.; P.-Albouy, A.; Perez-Omil, J. *Chem. Mater.* **1999**, *11*, 3460.

2. Experimental Section

2.1. Materials. Dimethyl sulfoxide, chloroform (Aldrich), and ω-tricosenoic acid (CH_2═$CH-(CH_2)_{20}-COOH$) (Interchim; Montluçon, France) were used as received and the films were built on a homemade LB trough filled with Millipore-grade water (resistivity higher than 18 MΩ·cm).

2.2. Synthesis. The synthesis of the platinum nanoparticles capped with mercaptoaniline molecules is described in detail elsewhere:[7] it provides particles with an average diameter of 1.5−2.0 nm that can be dissolved in dimethyl sulfoxide: the solutions presently used have a concentration of 0.5 mg/mL.

2.3. LB Films Elaboration. A difficulty arises from the fact that DMSO is miscible in water so that the solutions cannot be used as such. This problem is circumvented by adding 1 mL of chloroform to 0.5 mL of the DMSO solution just before spreading. For the study of mixed films containing ω-tricosenoic acid and platinum nanoparticles, the spreading solution was prepared by mixing 0.5 mL of DMSO solution with ≈100 μL of a 6.6 × 10^{-4} M solution of fatty acid in chloroform, the volume being completed to 1.5 mL by adding chloroform. Therefore, the ratios DMSO to chloroform in the spreading solutions were identical for the elaboration of pure and mixed films.

The transfer of pure films (containing only functionalized platinum nanoparticles) was performed horizontally as follows: the solid substrate was introduced into the subphase before spreading and positioned as close as possible from the air/water interface (about 0.1 cm) and then the trough was slowly emptied after the formation of the film (film pressure: 4 mN/m) until deposition on the substrate. The entire process must be repeated to deposit additional layers. The mixed films were transferred vertically at a surface pressure of 30 mN/m with a transfer speed of 0.3−0.5 cm/min.

2.4. Characterization. Infrared spectra were recorded on films deposited onto calcium fluoride slides using a 1720 X Perkin-Elmer FTIR spectrometer (4-cm^{-1} resolution). X-ray measurements were performed either on LB films transferred onto ultrathin silicon slides or on bulk powder held in 0.3-

10.1021/cm001183r CCC: $20.00
Published on Web 04/03/2001

mm glass capillaries. In both cases, the diffraction pattern is recorded onto photostimulable imaging plates using a transmission geometry: this is a highly sensitive procedure that requires much less materials than conventional $\theta-2\theta$ diffractometry. For electrical measurements, LB films are transferred onto glass plates provided with interdigital gold electrodes; the electrodes consist of 10 finger pairs with width and spacing of 150 μm and 50 nm in thickness; gold adhesion is promoted by a treatment of the glass surface with (3-mercaptopropyl)-trimethoxysilane. The dc electrical properties were measured with a programmable 617 Keithley electrometer. The temperature-dependent measurements were performed under primary vacuum, the samples being positioned in a hollow frame and cooled by liquid nitrogen circulation. AFM measurements were carried out with a nanoscope IIIa (Digital Instruments) in the tapping mode in air and room temperature on films transferred onto freshly cleaved mica foils. Electron microscopy images were recorded on a scanning transmission electronic microscope from VG AB501, in annular dark field mode.

3. Results and Discussion

3.1. Langmuir Films of Pure Platinum Nanoparticles and Platinum Nanoparticles Mixed with a Fatty Acid. The average molecular weight for each preparation needs to be evaluated before preparing the spreading solution to calculate the area per particle at the air−water interface. The molecular weight is essentially defined by the number of platinum atoms per particle. It is first related to the average size of the platinum core, which is determined by a shape analysis of the X-ray wide-angle diffraction lines as explained elsewhere.[8] Various polyhedra can be used, keeping in mind that the line profile is not very sensitive to this choice. For the sake of simplicity, we assumed in a previous publication that the aggregates were cubic in shape:[7] in this way, the diffraction data could be adjusted using essentially cubes with edges 3a and 4a, where $a = 0.392$ nm is the cubic parameter. In the present paper, we suppose the agregates to be cuboctahedral, which is more realistic.[8−10] The main consequence of this choice is a reduction by 0.2 nm on the evaluation of the thickness of the organic layer coating the particles, now found equal to 0.7 nm (see Table 1). The small contribution of the organic part to the molecular weight of the functionalized particles is readily calculated from elemental analysis.[7] The compression isotherms presented in Figure 1 have been recorded by steps of 2 mN/m and correspond to preparations characterized by a different average core diameter. The collapse of the film proceeds very slowly. It seems essentially located at the mobile barrier where an accumulation of matter is clearly observed when the surface pressure reaches 6 mN/m. Compared to results reported in the literature,[4,6] this value is quite low; however, most of the papers reporting on LB films based on encapsulated particles deal with aggregates bigger in size and bearing a purely hydrophobic organic shell. Table 1 reports structural features and the area per particle at 2 mN/m for different syntheses exhibiting slightly different sizes. A good correlation is observed between the diameter of the particle core and the area per particle.

Table 1. Structural Data Evaluated for Different Batches of Platinum Functionalized Nanoparticles[a]

batch	interparticle distance[b] (nm) (bulk)	averaged core diameter[c] (nm)	organic layer thickness[d] (nm)	area per particle at 2 mN/m[e] (nm^2)	interparticle distance[f] (Langmuir film) (nm)
1	3.28	2.03	0.62	10.66	3.68
2	3.48	2.03	0.72	9.81	3.53
3	3.50	1.97	0.76	7.40	3.07
4	3.21	1.91	0.65	7.66	3.12
5	3.34	1.87	0.73	6.75	2.93
6	3.34	1.87	0.73	7.14	3.01
7	3.03	1.67	0.68	4.8	2.47

[a] First column indicates the interparticle distance recorded in bulk materials. Second column is the averaged core diameter of the particles. The last three columns report respectively the thickness of the organic crown, the area per particle at the air−water interface (2 mN/m), and the interparticle distance calculated from these values (see text). [b] Deduced from small-angle X-ray diffusion. [c] Deduced from wide-angle X-ray diffraction. [d] Evaluated from half the difference of the interparticle distance and the averaged core diameter. [e] Calculated from compression isotherm. [f] Interparticle distance deduced from the area per particle.

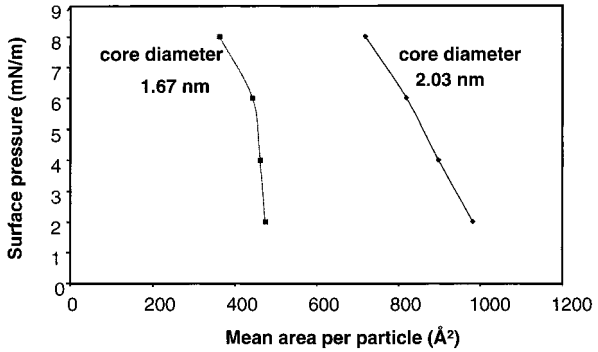

Figure 1. Compression isotherm recorded at 19 °C, for 4-mercaptoaniline functionalized nanoparticles having various core diameters.

The aging of the particles suspension has been evidenced by recording the pressure isotherm as a function of time. It has been observed that the area per particle at 2 mN/m decreases by ≈50% within 3 months. This process can be ascribed to a chemical degradation of the organic part in solution previously observed in the bulk material.[7] From the area per particle recorded on freshly prepared solution, an average interparticle distance in the monolayer can be estimated assuming that each particle occupies a circular area of diameter ϕ. The values of ϕ calculated in this way are reported in Table 1 and show a good correlation with the interparticle distance determined on bulk powders by small angle X-ray scattering. For each preparation, the difference between these two distances are quite close and lies within ±0.5 nm; it suggests that the Langmuir film formed at low pressure essentially consists of monoparticle thick material. This point is supported by AFM measurements recorded on a horizontally transferred monolayer (see below) as shown in Figure 2a. At low pressure (4 mN/m), most of the material is homogeneous with a small number of holes. The thickness has been determined using the bottom of the holes (mica) as reference height and has been found equal to 2.95 nm. This determination is close to the interparticle distance found by small-angle X-ray diffraction (see Table 1). Some thicker islands correspond to local

(8) Gnutzmann, V.; Vogel, W. *J. Phys. Chem.* **1990**, *94*, 4991.
(9) Rodriguez, A.; Amiens, C.; Chaudret, B.; Casanove, M.-J.; Lecante, P.; Bradley, J. S. *Chem. Mater.* **1996**, *8*, 1978.
(10) Schmid, G.; Morun, B.; Malm, J.-O. *Angew. Chem Int. Ed. Engl.* **1988**, *28*, 778.

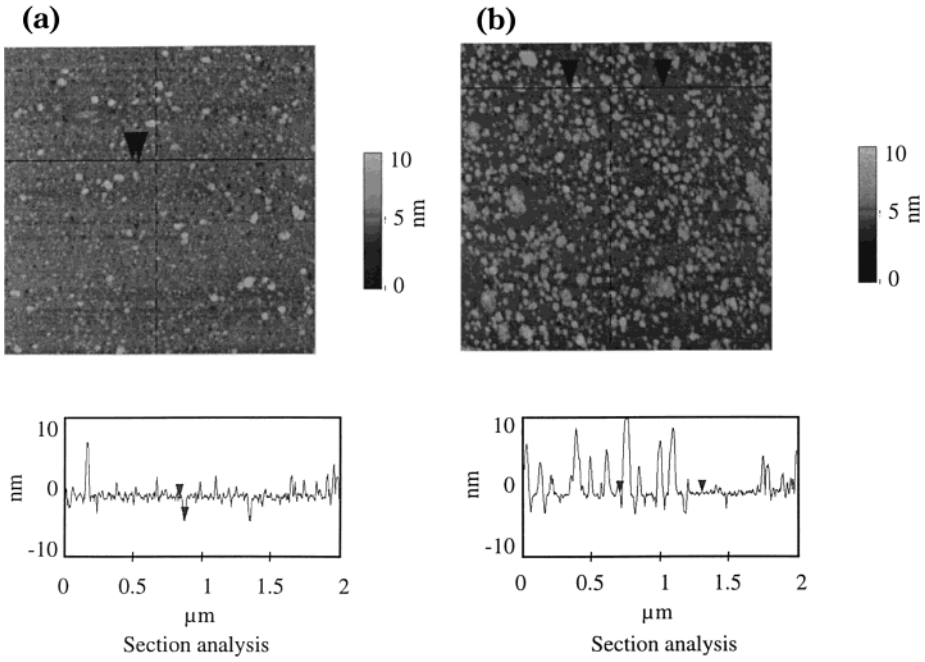

Figure 2. AFM images recorded on one layer of pure functionalized platinum nanoparticles transferred horizontally at a pressure of 4 mN/m (a) and 10 mN/m (b). Section analysis recorded from each picture is reported. The vertical distance between the arrows on section analysis of Figure 2a is 2.95 nm.

accumulation of few particles that are expelled from the monolayer. The thicker parts are much more numerous at higher pressures as shown in Figure 2b for a film transferred at 10 mN/m where the area per particle at the air−water interface is reduced by more than 50% compared to the area calculated at low pressures. The section analysis recorded from both experiments illustrate the effect of pressure on the quality of the films: the material transferred at 10 mN/m exhibit a higher density of thicker region compared to the material transferred at 4 mN/m. The good quality of the Langmuir film at low pressures is clearly confirmed by STEM. Figure 3 shows two images of a Langmuir film of pure functionalized platinum nanoparticles horizontally transferred on a microscope grid at a pressure of 4 mN/m. It confirms that the film is essentially a monolayer; defects mostly consist in holes (white area); some darker zones may be attributed to particles expelled from the monolayer.

Aiming at the improvement of both the stability of the film and its ability to be transferred, the formation of Langmuir films based on a mixture of a fatty acid (ω-tricosenoic acid) and the platinum nanoparticles has been investigated. The concentration in fatty acid is such that it should cover about half the surface at low pressure. A very slow compression rate (typically 0.02 nm^2/particle/mn) is necessary to obtain reproducible results. Figure 4 shows the isotherm obtained in this way (a) and after subtraction of the estimated fatty acid contribution (b) (it is assumed that the area per acid molecule in the mixed film is the same as that in the pure film of ω-tricosenoic acid): in these conditions, the area per particle at 30 mN/m in the mixed film is about the same as the one found in the film based on pure nanoparticles at 6 mN/m. It can be thus concluded that the nanoparticles are not expelled from the air/water interface, even at high pressures. X-ray data on transferred films strongly suggest that the Langmuir film is made up of separated fatty acid and nanoparticles domains.

3.2. Infrared Characterization. The infrared characterization concerns the mixed LB films. The IR spectra of Figure 5a is a simple overlaying of the IR spectrum of the functionalized nanoparticles (Figure 5c) and that of the fatty acid (Figure 5d). Therefore, it demonstrates that no significant chemical interaction occurs between the carboxylic function of the fatty acid and amine functions of the functionalized particle. Indeed, in such a case additional absorption bands due to ammonium and carboxylate groups should be visible. The low basicity of the amine functions surrounding the particles is presumably responsible for this fact. However, a more detailed observation reveals some differences that concern the fatty acid. Indeed, on spectrum (d) the alkyl chains appear as a doublet at 1463 and 1472 cm^{-1} (see the insert in Figure 5) and the carboxylic function at 1701 cm^{-1} whereas on spectrum (a) (mixed film), the absorption band characteristic for the alkyl chains is a single peak located at 1468 cm^{-1} and the carboxylic function is located at 1709 cm^{-1}. These differences can be attributed to a slight perturbation of the fatty acid packing in the mixed film by the nanoparticles. Indeed, it is known that the modification of the CH_2 wagging peaks from a doublet into a singlet is very sensitive to slight modification of the crystal structure of the fatty acid phase.[11−13] Moreover, the higher frequency of the carboxylic function probably reflects lower hydrogen bonding.[11]

The ability to remove the fatty acid from the LB films by chloroform washing has also been verified by

(11) Nakamoto, K.; In *Infrared and Raman Spectra of Inorganic and Coordination Compounds*, 5th ed; John Wiley & Sons: New York, 1997.

(12) Leloup, J.; Maire, P.; Ruaudel-Teixier, A.; Barraud, A. *J. Chim. Phys.* **1985**, *82*, 695.

(13) Belbeoch, B.; Roulliay, M.; Tournarie, M. *J. Chim. Phys.* **1985**, *82*, 701.

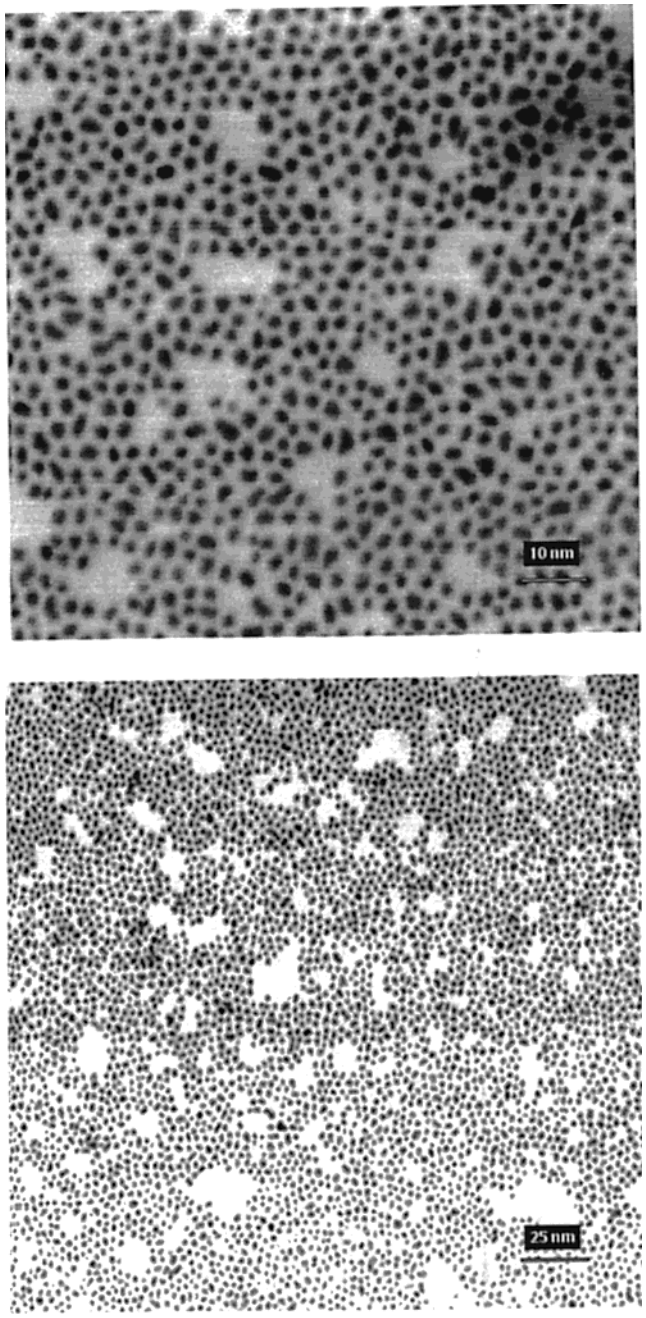

Figure 3. Scanning transmission electron microscopy images recorded on a monolayer of pure functionalized platinum nanoparticles transferred horizontally at a pressure of 4 mN/m. Two different magnifications are given.

this technique. Indeed, the carboxylic function is not visible on the spectrum after washing (Figure 5b), which confirms that the fatty acid has been essentially removed. On the basis of the intensities of the C−H stretching modes located at 2922 and 2853 cm^{-1}, the percentage of removed fatty acid is roughly estimated to be 90% (not shown). Finally, we also found that this treatment leads to the elimination of 5−10% of the functionalized particles, which are probably isolated objects embedded in fatty acid domains.

3.3. X-ray Characterization. As quoted above, some relevant structural features for the bulk material have been determined by small- and wide-angle X-ray scattering. Indeed, because of the high scattering power of platinum, this method can also be applied to LB films

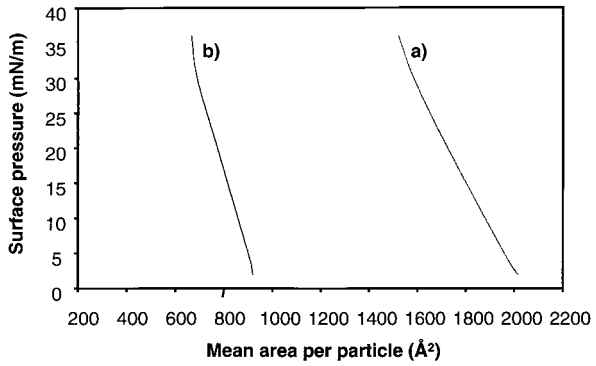

Figure 4. Compression isotherm of mixed film based on functionalized platinum nanoparticles and ω-tricosenoic acid. The platinum nanoparticle core diameter was 2.03 nm (same particle as in Figure 2). Isotherm (a) reports the area per particle including the contribution of the amphiphilic molecule. Isotherm (b) reports the area per particle after subtraction of the contribution due to the fatty acid.

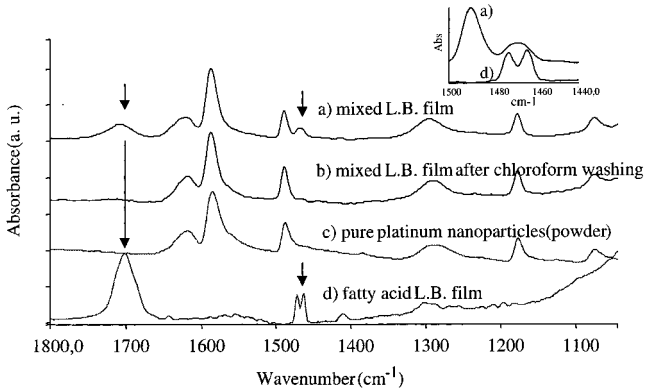

Figure 5. Infrared spectra of five-layers thick LB films based on functionalized platinum nanoparticles and fatty acid before (a) and after (b) washing with chloroform. Spectra (c) correspond to the LB film of pure fatty acid and spectra (d) to the bulk platinum nanoparticles. The arrows reported on the spectra indicate the fatty acid absorption (see text). An enlarged view of the 1440−1500-cm^{-1} region (aliphatic chains) is given in the insert.

Table 2. Comparison of the Interparticle Distance in the Bulk Material and in the Mixed LB Films for Two Different Core Diameter Nanoparticles

batch	interparticle distance (bulk) (nm)	interparticle distance (LB) (nm)	difference bulk/LB (nm)
4	3.21	3.7	0.49
7	3.03	3.5	0.47

consisting in a few deposited layers. Table 2 reports determinations performed on two mixed L−B samples. It is readily seen that the interparticle distance is higher than that in the bulk. This is probably due to the presence of some fatty acid molecules dispersed between the particles. However, most of the acid is found in well-defined domains as evidenced by the observation of a strong diffraction peak at 0.42 nm. The interparticle distance is almost unaffected by chloroform washing but the peak at 0.42 nm is completely removed. A parameter not presented here is the correlation length, which indicates the degree of positional order.[7] Correlation lengths equal to twice the interparticle distance are found in the bulk or in the LB films. Positional order is thus only short-range, which can be related to the fact that the particle size distribution is not single-dispersed.

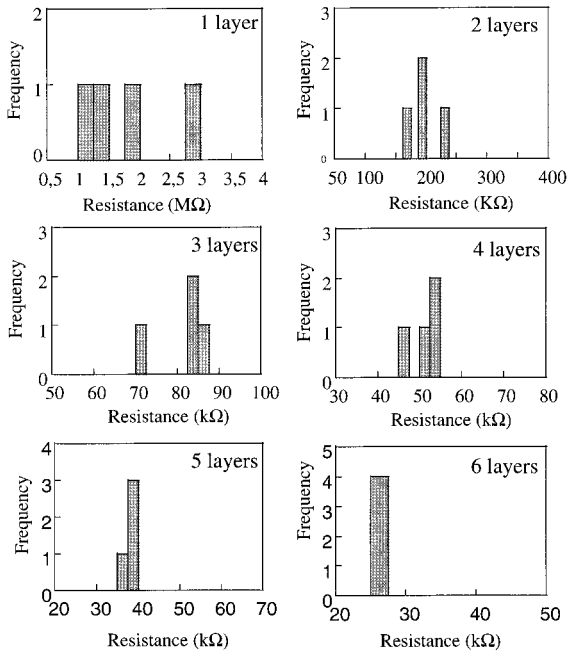

Figure 6. Histograms of resistance values recorded for one to six layers (a to f) deposited horizontally. The particle core diameter was 1.67 nm.

3.4. Electrical Measurements on Langmuir−Blodgett Films of Pure Platinum Nanoparticles and Platinum Nanoparticles Mixed with a Fatty Acid. 3.4.1. LB Films from Pure Platinum Nanoparticles. The electrical measurements have been performed on films horizontally deposited; the number of layers ranges from one to six and in each case four samples have been prepared. The average core diameter of the particles used for these experiments was 1.67 nm. Figure 6 represents the resistance histograms obtained at 298 K. It shows that the resistance level decreases dramatically as the number of layers increases while the scattering of the data becomes much narrower. Figure 6 reports the film conductivity as a function of the number of layers: a plateau is observed above 3−4 layers, indicating a conductivity of $\approx 2.5 \times 10^{-2}$ S·cm^{-1}. It is suspected that the conductivity is lower for lower thickness because of the presence of defects in the film. The above-mentioned conductivity is much lower than that for bulk platinum (9.5×10^{5} S·cm^{-1}) which is consistent with numerous results published in the literature and reflects quantum size effects. The size dependence of electrical properties has been already studied on ultrathin evaporated metal films[14−16] and more recently on materials based on encapsulated nanoparticles.[17−19] The temperature dependence of the conductivity has been investigated from −135 to 25 °C on a one-layer-thick sample (average particle diameter: 2.03 nm). An Arrhenius plot gives an activation energy of 80 meV (Figure 8). This value is difficult to compare directly with results reported in the literature as it is known to depend on the metal, the particle size, the interparticle distance, and probably the chemical characteristic of the organic crown.[15,17−19] However, it lies in the same range as those mentioned elsewhere for palladium and gold aggregates.[19−21] The electrostatic model developed by Abeles et al.[15] relates this energy to the radius of the particle, the interparticle distance (edge to edge), and the relative permittivity of the surrounding media of the particle. Brust et al. exploited this relation and found good agreement between this model and their experimental results on gold-encapsulated nanoparticles with 2.2- and 8.8-nm core diameters.[17] As relative permittivity (ϵ), they took a value of 2 corresponding to saturated hydrocarbons. Using our experimental data and the above-mentioned relation, a relative permittivity of 5.3 is found: this value is close to those reported for similar molecules such as benzenethiol (4.26) or aniline (7.06). This suggests that our nanoparticles films behave as a network of individual metal nanoparticles exhibiting nonmetallic electronic properties.

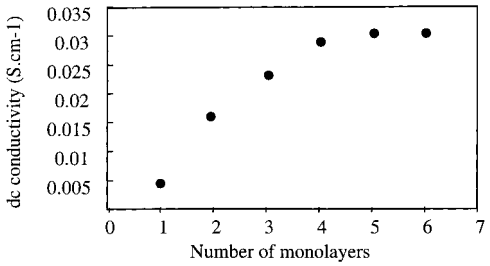

Figure 7. Conductivity as a function of the number of layers deposited. These values are calculated from the averages of the data reported on histograms from Figure 5.

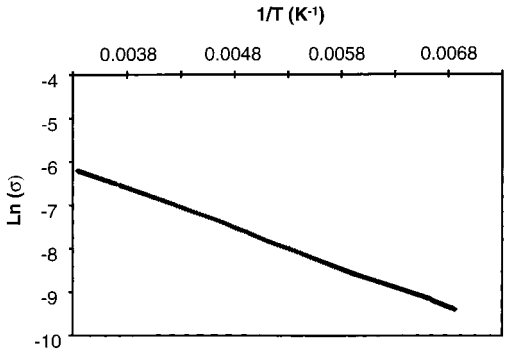

Figure 8. Arrhenius plot of one layer of a pure 2.03-nm core diameter platinum nanoparticle transferred horizontally. The activation energy calculated from these data is 80 meV.

3.4.2. LB Films of Platinum Nanoparticles Mixed with a Fatty Acid. The average diameter of the particles used in these experiments was 2.03 nm. The conductivities calculated for samples with one and three layers are respectively 5.4×10^{-3} and 1.5×10^{-2} S·cm^{-1}. This result shows that the electrical percolation of nanoparticles is not strongly affected by the fatty acid despite its effect on the interparticle distance, which increases by ≈0.5 nm; indeed, studies by Terrill et al.[22] reporting on the effect of alkyl chain on the dc conductivity for alkylthiol-encapsulated gold nanoparticles

(14) Neugebauer, C. A.; Webb, M. B. *J. Appl. Phys.* **1962**, *33*, 74.
(15) Abeles, B.; Cheng, P.; Couts, M. D.; Arie, Y. *Adv. Phys.* **1975**, *24*, 407.
(16) Barwinsky, B. *Thin Solid Films* **1985**, *128*, 1.
(17) Brust, M.; Bethell, D.; Schiffrin, D. J.; Kiely, C. J. *Adv. Mater.* **1995**, *7*, 795.
(18) Snow, A. W.; Wohltjen, H. *Chem. Mater.* **1998**, *10*, 947.
(19) Brust, M.; Bethell, D.; Kiely, C. J.; Schiffrin, D. J. *Langmuir* **1998**, *14*, 5425.
(20) Schmid, G.; Chi, L. F. *Adv. Mater.* **1998**, *10*, 515.
(21) Simon, U.; Flesh, R.; Wiggers, H.; Schön, G.; Schmid, G. *J. Mater. Chem.* **1998**, *8*, 517.

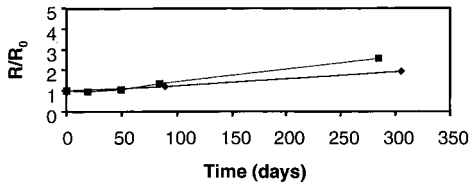

Figure 9. Variation of the resistance of LB films based on functionalized platinum nanoparticles as a function of time (two different samples).

show a decrease by a factor of 10^{-2} when increasing the chain length by four carbon atoms.

Removal of the fatty acid by chloroform washing weakly modifies the resistance value (by 5−20%). This result is consistent with results obtained from IR and X-ray measurements as the fatty acid is essentially present as crystallized domains whose removal poorly affects the nanoparticle content in the material. The electrical stability of the materials has been evaluated. As shown in Figure 9 the resistance exhibits satisfying long-term stability. The small drift could be related to the chemical evolution of the organic crown observed upon aging in the bulk material.[7] This point is currently under investigation.

4. Conclusion

The results presented here demonstrate the ability of platinum nanoparticles functionalized by 4-mercaptoaniline to form Langmuir films. In the case of pure films, the collapse pressure is quite low, which is probably related to both the polar properties of the organic shell and the small particle size. The pure film is found to be essentially a monolayer at low pressures as shown by the area per particle, AFM, and STEM characterizations. A good correlation is observed between the area per particle at the air−water/interface and the size of the core of the nanoparticles. The interparticle distance deduced from these area measurements is in good agreement with the value found in the corresponding bulk material. Mixing with a true amphiphilic moiety increases the stability of the film, which remains essentially a monolayer up to pressures as high as 30 mN/m. The pure Langmuir film can only be transferred horizontally by trough draining. The electrical conductivity becomes independent of the film thickness beyond three to four deposited layers and found to be $\approx 10^{-2}$ S·cm^{-1}. Vertical deposition is readily achieved with the mixed film and the transfer ratio is close to unity. Conductivity measurements show that the electrical percolation between particles is not strongly disturbed by the presence of fatty acid. Preliminary experiments indicate that removal of the acid by chloroform washing poorly affects the level of conductivity. These films exhibit good electrical stability over long periods of time. It is shown in a forthcoming paper how the amine functionality of the platinum nanoparticles can be exploited for overgrafting with various molecules.

Acknowledgment. The authors thank Dr. J. P. Bourgoin for the AFM characterization and Dr. O. Stephan for the STEM images.

CM001183R

(22) Terrill, R. H.; Postlethwaite, T. A.; Chen, C.−H; Poon, C.-D.; Terzis, A.; Chen, A.; Hutchinson, J. E.; Clark, M. R.; Wignall, G.; Londono, J. D.; Superfine, R.; Falvo, M.; Johnson, C. S.; Smulski, E. T.; Murray, R. *J. Am. Chem. Soc.* **1995**, *117*, 12537.